Original Article

Hydrogel and neural progenitor cell delivery supports organotypic fetal spinal cord development in an *ex vivo* model of prenatal spina bifida repair

Journal of Tissue Engineering
Volume 11: 1–15

DOI: 10.1177/2041731420943833
journals.sagepub.com/home/tej
SAGE

Juan C Biancotti[1*], Kendal A Walker[2*], Guihua Jiang[2], Julie Di Bernardo[2], Lonnie D Shea[3] and Shaun M Kunisaki[1,4]

Abstract

Studying how the fetal spinal cord regenerates in an *ex vivo* model of spina bifida repair may provide insights into the development of new tissue engineering treatment strategies to better optimize neurologic function in affected patients. Here, we developed hydrogel surgical patches designed for prenatal repair of myelomeningocele defects and demonstrated viability of both human and rat neural progenitor donor cells within this three-dimensional scaffold microenvironment. We then established an organotypic slice culture model using transverse lumbar spinal cord slices harvested from retinoic acid–exposed fetal rats to study the effect of fibrin hydrogel patches *ex vivo*. Based on histology, immunohistochemistry, gene expression, and enzyme-linked immunoabsorbent assays, these experiments demonstrate the biocompatibility of fibrin hydrogel patches on the fetal spinal cord and suggest this organotypic slice culture system as a useful platform for evaluating mechanisms of damage and repair in children with neural tube defects.

Keywords

Myelomeningocele, spina bifida, neural tube defects, organotypic, slice culture, hydrogels, fetal surgery

Date received: 2 May 2020; accepted: 29 June 2020

Introduction

Myelomeningocele (MMC) is a severe, prenatally diagnosed form of spina bifida resulting from failed fusion of the caudal region of the neural tube during embryonic development. The diagnosis is synonymous with substantial and permanent disabilities secondary to leg weakness and paralysis, hydrocephalus, cognitive impairment, bladder and bowel dysfunction, and orthopedic abnormalities.[1]

Given the unfortunate prognosis of the MMC fetus, one option for pregnant mothers is to undergo *in utero* primary closure of the neural tube defect at 25 weeks' gestation in an attempt to mitigate the secondary injury of the exposed spinal cord.[2,3] Although the procedure has shown clinical benefit in a randomized trial,[4] the operation is highly invasive, induces preterm labor, and has mixed long-term neurologic outcomes. Another drawback of current prenatal repair techniques is that they do not address the primary and chronic secondary spinal cord damage that has already occurred.[5] The ability to provide MMC children with treatment options that can better enhance the regenerative capacity of already damaged spinal cord tissue is needed.

Tissue engineering–based techniques that enable complete tissue coverage of spina bifida defects while actively facilitating spinal cord regeneration have gained traction as an alternative treatment strategy in experimental models.[5–8] Unfortunately, the testing of these approaches has been

[1]Division of General Pediatric Surgery, Department of Surgery, Johns Hopkins University, Baltimore, MD, USA
[2]Section of Pediatric Surgery, Department of Surgery, University of Michigan, Ann Arbor, MI, USA
[3]Department of Biomedical Engineering, University of Michigan, Ann Arbor, MI, USA
[4]Fetal Program, Johns Hopkins Children's Center, Baltimore, MD, USA

*Shared first authorship.

Corresponding author:
Shaun M Kunisaki, Fetal Program, Johns Hopkins Children's Center, 1800 Orleans Street, Suite 7353, Baltimore, MD 21287-0005, USA.
Email: skunisa1@jhmi.edu

challenged by traditional fetal models of MMC repair, all of which have a number of shortcomings. For example, *in vivo* repair of MMC in fetal rodents is technically difficult to perform due to their small size and fragility.[7] There are also limitations in the number of fetuses that can be treated *in vivo* to avoid high risk of postoperative demise.[9] Moreover, affected pups do not routinely survive into the postnatal period to adequately evaluate treatment effect.[10] Fetal large animal models of MMC share many of the same challenges seen in rodent models and are very expensive to conduct.[11,12] The establishment of an *ex vivo* model that combines some of the advantages of animal models with those inherent with dissociated two-dimensional (2D) cell cultures may be an ideal and complementary research platform to explore the molecular and cellular aspects of MMC disease mechanism and repair, thereby representing an advance in this multidisciplinary field.

In this study, we sought to develop a novel, injectable hydrogel-based patch for use during fetal MMC surgical repair. We then aimed to evaluate the effect of these hydrogel constructs in an organotypic slice culture model of fetal MMC repair. Our hypothesis was that fibrin-based hydrogels would provide a supportive three-dimensional (3D) microenvironment for donor-derived neural progenitor cells of either human or rodent origin. Moreover, we speculated that hydrogel patches would be biocompatible with prenatal MMC spinal cord tissue and would facilitate ongoing neuronal differentiation and axonal regeneration in slice cultures.

Materials and methods

Fetal MMC rat model

This study was approved at the Johns Hopkins University and the University of Michigan under protocols RA19M88 and PRO00007385, respectively, in accordance with the National Institute of Health (NIH) Guidelines for the Care and Use of Laboratory Animals. To induce fetal MMC, timed-pregnant Sprague Dawley dams ($n=10$, Charles River, Wilmington, MA) were gavage fed 60 mg/kg of retinoic acid (Sigma-Aldrich, St. Louis, MO) on E10.5 as previously described.[10] On E21 (term = E22), the dams were deeply anesthetized, and all fetal pups (range, 8–12 per dam), regardless of sex, were harvested by a midline laparotomy (Figure 1(a) and (b)). Fetuses were euthanized by decapitation, and the spinal cords in those with isolated lumbosacral MMC ($n=60$) were removed *in toto* in sterile manner and immersed in ice-cold Hanks' balanced salt solution (HBSS) containing glucose (10 nM) and sucrose (75 nM; Figure 1(c)).

Organotypic slice cultures

The organotypic slice culture model was adapted from the interface method as described elsewhere.[13,14] Briefly, fetal spinal cords in affected pups were aligned and placed on a block supported with 1% agarose. The caudal portion was then sliced into 400 µm sections using a vibatrome (McIlwain Tissue Chopper; Ted Pella, Redding, CA; Figure 1(c)). Three to five transverse or longitudinal slices with intact topography were placed on top of the membrane inserts (PICM0RG50; Millipore, Burlington, MA) within 35 mm culture dishes (Figure 1(d)). The first group ($n=8$) of slices were encapsulated in a fibrin hydrogel patch (250 mL droplet) without cells. The second group ($n=8$) of slices were encapsulated in a 250-mL hydrogel droplet containing rat neural progenitors (1.25×10^5). The third group ($n=6$) of slices, which served as a control, received no hydrogel or cell treatment. One milliliter of medium containing DMEM with HEPES (50%; Gibco, Gaithersburg, MD), horse serum (25%; Gibco), and HBSS (25%; Gibco) was added to ensure coverage of each slice. Organotypic cultures were maintained for up to 14 days under standard conditions (37°C, 5% CO_2).

Hydrogel patches

Based on our prior studies[15] and work from others demonstrating increased neural fiber formation and delayed astrocytosis,[16,17] fibrin hydrogel patches (50–250 mL each) were generated by mixing human fibrinogen monomers (40 mg/mL; Calbiochem, Gibbstown, NJ), thrombin (50 U/mL; Sigma), and $CaCl_2$ (3.75 mM; Merck, Kenilworth, NJ). In a subset of human neural progenitor experiments, self-assembling peptide nanofiber hydrogels (Puramatrix™ 0.15%; 3D Matrix Medical, Waltham, MA) were also used per the manufacturer's instructions.

Neural progenitor cells

Approval for all human cell experiments was obtained from the Johns Hopkins University (IRB #202082) and the University of Michigan (IRB #38565). After written informed consent was obtained, human somatic cells were acquired from unused amniocentesis samples ($n=3$, 8–10 mL) collected from MMC ($n=1$) and normal ($n=2$) fetuses (mean gestational age = 25 weeks, two males and one female). Specimen donations were anonymous and would have otherwise been discarded as medical waste. The amniocytes were isolated and expanded in culture.[18] Integration-free induced pluripotent stem cells (iPSCs) were generated in our laboratory using a non-integrating, cytoplasmic Sendai virus (Cyto-Tune; Thermo Fisher, Waltham, MA) encoding for *OCT4, SOX2, KLF4*, and *cMYC* (Yamanaka factors), as previously described.[19] Individual colonies were subsequently picked mechanically and propagated on Matrigel (BD Biosciences, San Jose, CA). Alkaline phosphatase staining was performed using the AP substrate kit (Millipore) according to the manufacturer's instructions. Immunofluorescence staining

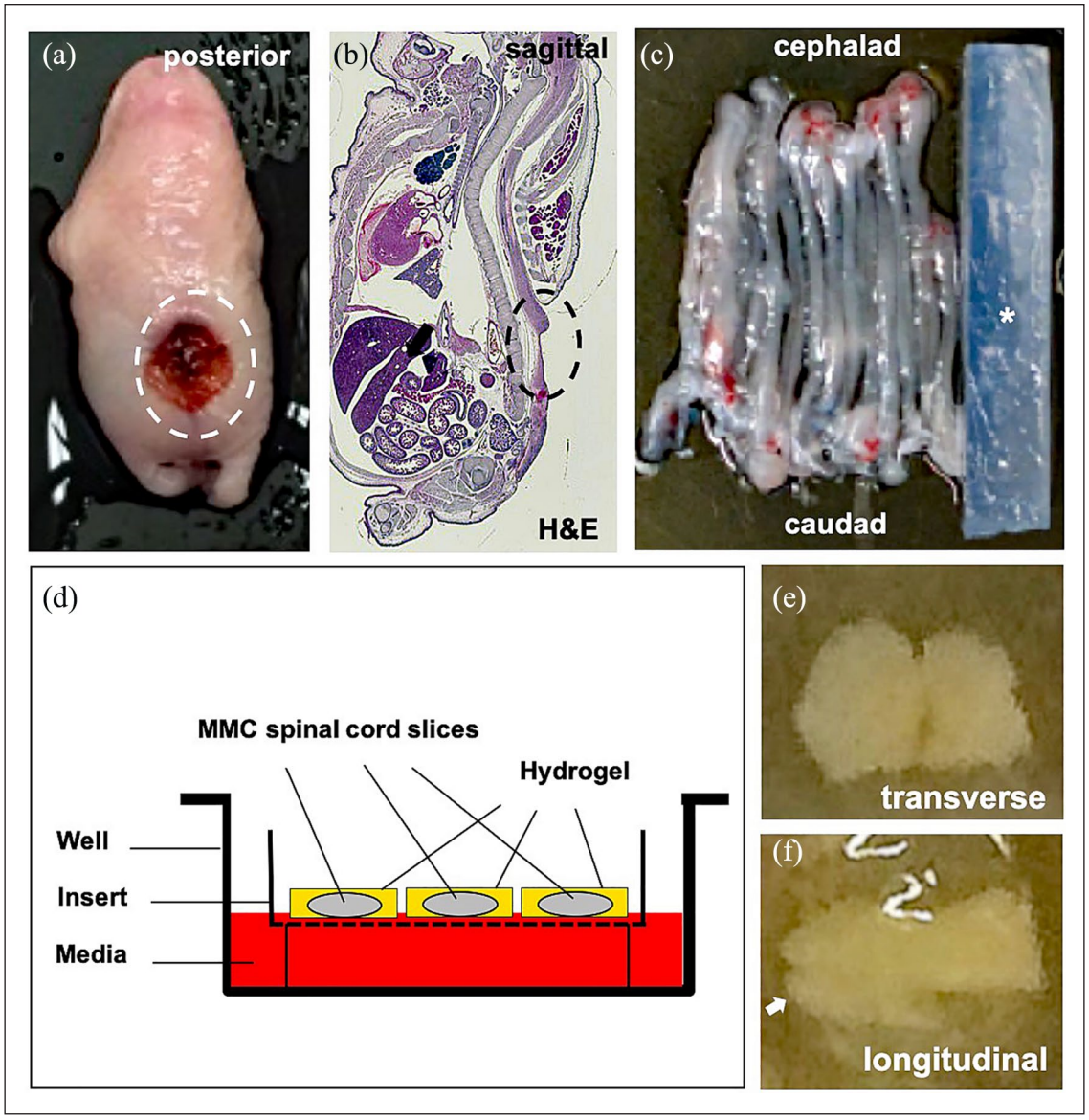

Figure 1. Organotypic slice culture rat model of fetal myelomeningocele (MMC) hydrogel patch treatment. (a) Gross inspection of representative lumbosacral defect (dotted oval) in a fetal MMC rat after maternal retinoic acid exposure. (b) H&E sagittal section through fetal MMC rat demonstrating lumbosacral defect (dotted oval, magnification: 4×). (c) Gross appearance of intact rat MMC spinal cords adjacent to an agarose block (asterisk). (d) Schematic view of MMC organotypic system showing spinal cord slices encapsulated within a hydrogel patch. Membrane inserts allow for nutrient absorption to ensure viability. No donor cells are depicted. (e) Representative transverse section (400 µm) of MMC lumbar spinal cord embedded in fibrin hydrogel on brightfield microscopy (day 0, magnification: 4×). Note the preservation of gross topography including median fissures. (f) Representative longitudinal section (400 µm) of MMC lumbar spinal cord embedded in fibrin hydrogel (day 0, magnification: 4×), white arrow = caudal end.

was used to assess pluripotency in established iPSC lines. Primary antibodies against NANOG (Abcam, Cambridge, MA), OCT4A (Santa Cruz, Dallas, TX), SOX2, SSEA3, SSEA4, TRA-1-60, and TRA-1-81 (Millipore) were used.

Differentiation of iPSCs into neural progenitors was conducted as previously described.[19] Briefly, neurospheres were created from iPSC clones derived from all three patients. Individual rosettes were re-plated into dishes containing neural stem cell media (Neurobasal media, B27 (Invitrogen, Carlsbad, CA), NEAA, GlutaMAX, and FGF-2). Neural progenitors were expanded and enriched using magnetic microbeads (Miltenyi Biotec, Gaithersburg, MD) conjugated with PSA-NCAM (Millipore) antibody. Karyotyping of neural progenitors was performed after five passages using the GTL-banding method on 20 metaphase preparations. To assess neural phenotype in 2D and 3D culture, the cells were evaluated by gene expression or fixed in 4% paraformaldehyde and stained with primary

antibodies at 96 h. Confocal imaging was performed using a Nikon A-1 confocal microscope (Melville, NY). The cells (5×10^5/mL) in hydrogel suspension were also assessed by live/dead assay (Molecular Probes, Thermo Fisher) at 8 and 24 h. Percent viability was calculated in a blinded fashion from six random images at each time point using ImageJ (NIH, Bethesda, MD).

Rat fetal neural progenitors were purchased from a commercial vendor (GSC-8010; GlobalStem, Rockville, MD) or isolated from fetal Sprague Dawley rat central nervous tissue. At passage 4, the cells were labeled with mKate red fluorescence protein (RFP) based on a lentivirus driven by a synapsin promoter (IncuCyte; Essen Biosciences, Ann Arbor, MI; multiplicity of infection = 1). Immunohistochemical detection of donor neural cells within slice cultures was assessed using an RFP antibody (Thermo Fisher).

Immunostaining

All spinal cord tissue was fixed in 4% paraformaldehyde prior to immunostaining using the following primary antibodies: nestin (1:800, Cat. No. MAB5326; Millipore), musashi-1 (MSI1; Millipore), b-III tubulin (Tuj1, 1:800, Cat. No. Ab107216; Abcam), glial fibrillary acidic protein (GFAP, 1:500; Cell Signaling, Danvers, MA), caspase 3 (Cas3, 1:100; Millipore), Ki67 (1:200; Millipore), oligodendrocyte transcription factor (OLIG2; Thermo Fisher), NeuN (Millipore), microtubule-associated protein-2 (MAP2, 1:1000; Thermo Fisher), and NF200 (Sigma). Three random areas of tissue were imaged using a multiphoton microscope (Olympus FV1000, Waltham, MA) and converted into an RGB stack after tracing of total tissue area. Degree of staining was quantified in a blinded fashion based on the optical density method as described elsewhere.[20,21] The densities were calculated based on minimum and maximum color thresholds for each section using ImageJ.

Quantitative gene expression

Relative gene expression of spinal cord tissue was analyzed by quantitative reverse transcription polymerase chain reaction (qPCR). Total RNA was extracted from explants using a MagMAX-96 Total RNA Isolation Kit (Life Technologies, Carlsbad, CA) and MAG Max Express (Applied Biosystems, Foster City, CA). RNA quantity and quality were determined spectrophotometrically using a NanoDrop 2000 spectrophotometer (Thermo Fisher). Reverse transcription was conducted using the SuperScript VILO kit (Invitrogen) according to the manufacturer's protocol. Finally, qPCR was performed using Fast SYBR Green Master Mix (Applied Biosystems) and an AB-Quant Studio3 real-time PCR machine (Thermo Fisher). PCR primers were designed with Primer-BLAST (NIH; see Supplemental Table), and *GAPDH* was used as a reference gene for the normalization of target gene expression using the $2^{-\Delta\Delta Ct}$ method.

Neurotrophic factor analysis

Enzyme-linked immunoabsorbent assays (ELISA; Merck Millipore) were used to measure brain-derived neurotrophic factor (BDNF), neurotrophin-3 (NTF3), and neurotrophin-4/5 (NTF4) levels in slice cultures. These specific neurotrophic factors were measured given their association with the promotion of corticospinal axon growth and immunomodulatory properties.[22–24] ELISAs were performed twice on pooled slice cultures within a single dish according to the manufacturer's instructions, and concentrations were normalized to total protein for each sample.

Statistical analyses

Quantitative data were presented as mean ± standard error. Data were analyzed by the Mann–Whitney test or one-way analysis of variance with post hoc testing by Kruskal–Wallis correction for multiple comparisons, as appropriate, using Prism 8 (GraphPad, La Jolla, CA). The results were considered to be statistically significant if $p < 0.05$.

Results

3D hydrogel surgical patches support human neural progenitors

Human amniotic fluid cells were isolated from three fetuses, including one with MMC, and were successfully reprogrammed into iPSCs using non-integrating Sendai virus. Under standard stem cell media conditions, amniocytes uniformly began to aggregate while reducing cytoplasmic volume and losing spindle-shaped morphology. After 28 days, there were multiple candidate iPSC colonies with well-defined borders and high nuclear-to-cytoplasm ratios from all patients (Figure 2(a)). Morphologically distinct colonies expressed high levels of alkaline phosphatase (Figure 2(a), inset), and immunofluorescence staining of iPSCs revealed uniformly high expression of several pluripotency markers, including NANOG, OCT4, SOX2, SSEA3, SSEA4, TRA-1-60, and TRA-1-81.

Human iPSCs were then exposed to neural differentiation culture conditions. Neurospheres attached and formed neural rosettes typical of neuroepithelial cells within 7 days in adherent culture. All tested neural progenitor cell lines maintained a normal karyotype without clonal aberrations (Figure 2(b)). Directed differentiation in the neural lineage was confirmed by positive staining for multiple neural progenitor markers, including SOX2, nestin, and MSI1 (Figure 2(c)), and by the presence of axonal projections over time by light microscopy. The cells expressed moderate

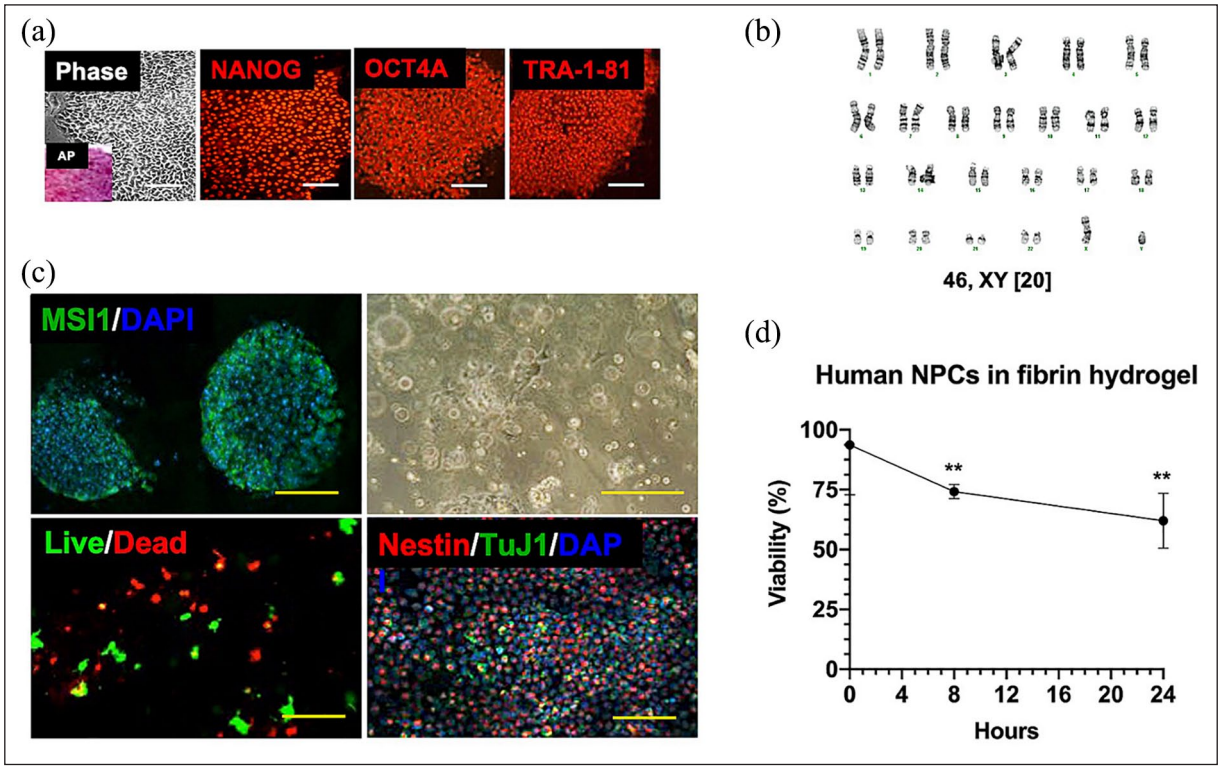

Figure 2. Neural progenitor hydrogel patch from human-induced pluripotent stem cells (iPSCs). (a) Representative colony morphology under phase microscopy with alkaline phosphatase (AP, inset) staining of iPSCs derived from amniotic fluid (left panel), and immunofluorescence profile of iPSCs using antibodies against several markers of pluripotency, including NANOG, OCT4A, and TRA-1-81 (middle and right panel, Cy3 secondary, magnification: 20×). Scale bars represent 100 mm. (b) Karyotype analysis of representative neural progenitor cells (NPCs; passage 8) derived from a male MMC fetus revealed 46,XY and no clonal aberrations. (c) Differentiation of iPSCs into neural progenitors as shown by immunofluorescent staining of neuroepithelial rosettes for musashi-1 (MSI1, FITC secondary, magnification: 40×, left upper panel). Nuclei were counterstained with DAPI. Scale bar represents 50 mm. Representative brightfield microscopy appearance of neural progenitors resuspended in fibrin hydrogel patches (magnification: 10×, right upper panel). Scale bar represents 200 mm. Demonstration of >60% 24-h NPC viability within hydrogel patch based on intracellular esterase activity (calcein-AM green) and plasma membrane integrity (ethidium homodimer-1 red, magnification: 40×, left lower panel). Scale bar represents 100 mm. Phenotypic characterization of neural progenitors by immunofluorescent staining showing abundant nestin-positive cells (Cy3 secondary) within hydrogel patches at 2 h. There was a relative paucity of TuJ1-positive cells (FITC secondary, magnification: 10×, right lower panel). Nuclei were counterstained with DAPI. Scale bar represents 500 mm. (d) Viability of human NPCs over time after resuspension in fibrin hydrogels based on intracellular esterase activity and plasma membrane integrity. Data are presented as mean ± SEM, $^{**}p \leq 0.01$ (Kruskal–Wallis compared to time 0), $n = 4$ independent biological replicates.

levels of TuJ1 but no detectable levels of GFAP, OLIG2, NANOG, and OCT4. Following resuspension of neural progenitors in hydrogel patches, gelation occurred within 15–30 min at 37°C. Neural progenitors within this 3D microenvironment demonstrated >60% viability when evaluated at 24 h based on intracellular esterase activity and plasma membrane integrity (Figure 2(d)). Immunofluorescent staining revealed predominantly nestin-positive cells, consistent with an immature neural progenitor cell phenotype.

Quantitative expression of various genes associated with neural development and differentiation showed that neural progenitors in hydrogel suspension did not alter RNA transcripts, including levels of *NES*, the gene encoding for nestin, which were comparable to those expressed in fetal brain positive controls (Figure 3(a)). The intermediate neural progenitor cell phenotype was confirmed by low *PAX6* expression in combination with negligible *MAP2, OLIG2*, and *GFAP* transcripts. Evidence of continued neurotrophic activity by neural progenitors resuspended in hydrogels was supported by significantly increased expression of *BDNF* and *NTF3* transcripts when compared with those in standard 2D culture (Figure 3(b)). Collectively, these data suggest that human neural progenitors derived from amniotic fluid iPSCs can survive and maintain neurogenic properties within 3D hydrogel matrices.

3D hydrogel patches are a vehicle for rat neural progenitors

Rat neural progenitors from all cell sources were successfully expanded and characterized prior to resuspension in

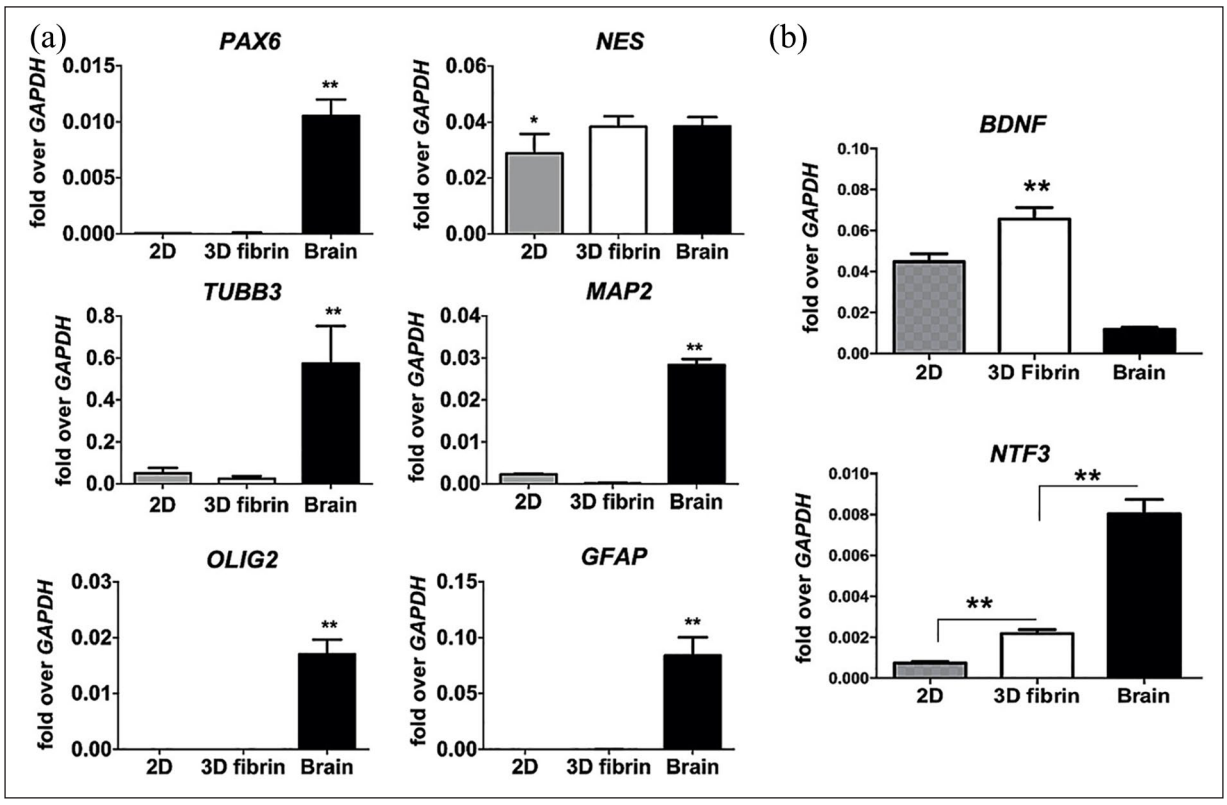

Figure 3. Gene expression and neurotrophic activity of human neural progenitors in 3D hydrogels at 96 h. (a) Representative quantitative gene expression data demonstrating relative specificity of neural progenitors derived from human iPSCs when compared to fetal brain positive controls. Placement of neural progenitors from 2D plates into 3D fibrin hydrogel suspensions did not alter gene expression, characterized by upregulation of *NES*, the gene encoding for nestin. Data were normalized relative to housekeeping gene (*GAPDH*) and are presented as mean ± SEM, $*p \leq 0.05$ and $**p \leq 0.01$ when compared to the other groups (Kruskal–Wallis), $n = 4$ independent biological replicates. (b) Quantitative gene expression showing relative neurotrophic activity of neural progenitors within 2D and 3D fibrin hydrogel microenvironments. There was upregulation in *BDNF* and *NTF3*, the genes encoding for brain-derived neurotrophic factor and neurotrophin-3, respectively. Human fetal brain RNA was used as a positive control, and data were normalized relative to housekeeping gene (*GAPDH*) and are presented as mean ± SEM, $*p \leq 0.05$ (Kruskal–Wallis), $n = 4$ independent biological replicates.

hydrogels (Figure 4(a)–(c)). Neural progenitors expressed both nestin and GFAP, and maintained >75% viability when resuspended in 3D culture at 8 and 24 h based on intracellular esterase activity and plasma membrane integrity. mKate2-labeled cells were visualized at 24 h (Figure 4(d)–(f)).

Slice culture model recapitulates development of the MMC spinal cord

Retinoic acid was given to pregnant rat dams to induce a posterior lumbosacral tissue defect in 66 (82.5%) of 80 term fetal pups (Figure 1(a) and (b)). The mean defect size was 7.9 mm × 5.4 mm. Lumbar spinal cord tissue harvested from affected rats was characterized by varying degrees of dorsal element injury. Nevertheless, representative immunohistochemistry showed a predominance of neuronal phenotypes in the expected topographical distribution within the gray matter of transverse sections (Figure 5(a)) and a relative paucity of astrocytes based on GFAP staining that were localized to the spinal cord periphery. The evaluation of slice cultures on day 1 demonstrated similar topography, which quantitatively revealed high levels of TuJ1, NeuN, and MAP2 and relatively low levels of GFAP and nestin at baseline (Figure 5(b)). There was no oligodendrocyte expression based on OLIG2. Evidence of baseline neurotrophic activity within slice cultures on day 1 was suggested by significant expression of *Bdnf* and *Ntf4* transcripts when compared with age-matched rat dorsal root ganglion positive controls (Figure 5(c)).

Hydrogel treatment supports neuronal maturation within slice cultures

Spinal cord slices cultured for 4, 7, or 14 days within hydrogels maintained cytoarchitectural integrity as shown by hematoxylin and eosin (H&E) staining (Figure 6(a)) with strong expression of both nestin and TuJ1 throughout

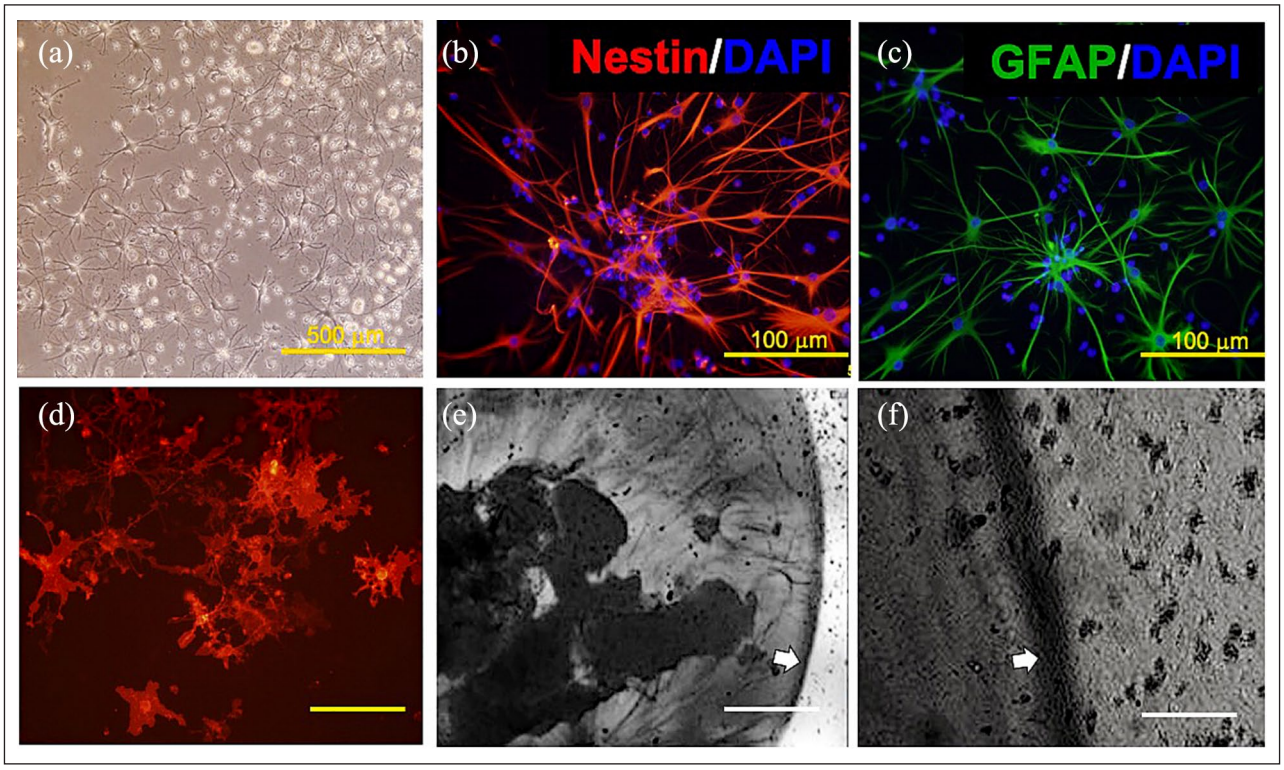

Figure 4. Characterization of donor rat neural progenitor cells. (a) Brightfield microscopy of rat neural progenitors in 2D culture (magnification: 10×). (b) Positive immunofluorescence staining of neural progenitors using antibodies against nestin (Cy3 secondary, magnification: 40×) at 24 h. (c) Positive immunofluorescence staining of neural progenitors using antibodies against GFAP (FITC secondary, magnification: 40×) at 24 h. Nuclei were counterstained with DAPI. (d) Representative appearance of mKate2-labeled neural progenitors within 3D hydrogel patch (magnification: 40×) at 24 h. Scale bar represents 50 mm. (e) Low-power light microscopy image showing rat neural cells contained within hydrogel patch (white arrow = patch edge, magnification: 10×). Scale bar represents 500 mm. (f) High-power light microscopy images of hydrogel patch edge (white arrow, magnification: 40×), $n = 8–10$ independent biological replicates for each experiment. Scale bar represents 100 mm.

the slice culture tissue (Figure 6(b)). Active outgrowth of axonal projections >500 mm from the tissue periphery was visualized in all groups by phase microscopy and by positive NF200 staining (Figure 6(c)). Although there was evidence of progressive hydrogel degradation over time by microscopy, approximately 25% of the remaining hydrogel was grossly visible on day 14.

Quantitative histopathologic alterations in neural cell phenotypes within transverse sections of slice cultures after 7 days (E21 + 7) or 14 days (E21 + 14) are summarized in Figure 7. Based on blinded analyses of immunohistochemistry images (Figure 7(a) and (b)), there were no significant changes in Ki67 and Cas3 expression over time (Figure 7(c) and (d)). There was increased expression of neuronal phenotypes at E21 + 14, including a statistically significant increase in TuJ1 after hydrogel treatment without cells (E21 + 14: 0.98 ± 0.11 vs E21 + 7: 0.51 ± 0.11, $p = 0.0125$, Figure 7(g)). Based on MAP2 and NeuN expression, neuronal maturation scores increased over time in all groups and was significantly increased in the hydrogel group compared to time-matched controls (Figure 7(h) and (i)). Conversely, GFAP expression declined by E21 + 14 and was statistically significant after hydrogel treatment without cells (E21 + 14: 0.32 ± 0.06 vs E21 + 7: 0.54 ± 0.11, $p = 0.0418$; Figure 7(j)). There were no statistical differences in GFAP expression among the three groups. Oligodendrocyte transcripts were undetectable in all cultures, and no mKate2-positive cells were visualized within slice cultures treated with hydrogel plus cells. Taken together, these data suggest acceptable biocompatibility of 3D fibrin hydrogels with MMC spinal cord slices in culture. Hydrogel treatment also correlated with enhancement of mature neuronal phenotypes when compared to controls without hydrogel.

Temporal increase in neurotrophic activity after hydrogel treatment

To evaluate the neurotrophic activity within slice cultures, ELISA was performed, which demonstrated a trend toward increased neurotrophic factor secretion within all slice cultures by E21 + 14. There was a statistically significant increase in NTF4 in slice cultures after hydrogel treatment with rat neural progenitors (E21 + 14: 107.6 ± 9.2 vs

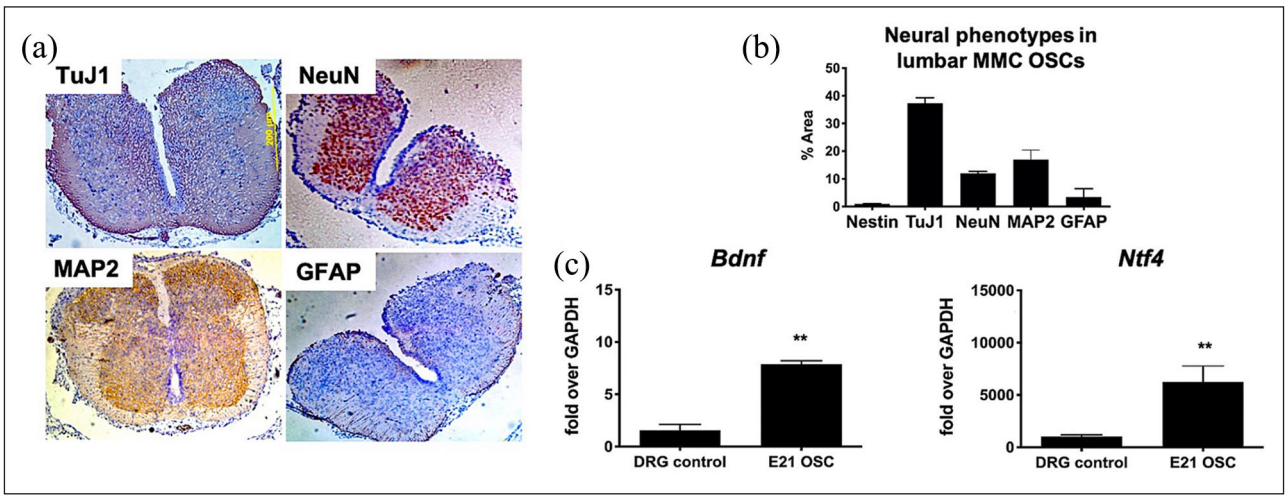

Figure 5. Baseline characteristics of cytoarchitecture and neural cell phenotypes within the myelomeningocele (MMC) lumbar spinal cord and slice cultures at E21. (a) Representative native MMC lumbar spinal (transverse sections) using TuJ1, NeuN, MAP2, and GFAP antibodies demonstrate a reduction in dorsal elements and predominance of neuronal phenotypes (magnification: 4×). (b) Quantification of neural phenotypes within transverse sections of fetal MMC organotypic slice cultures (OSCs) based on optical density (*y*-axis) calculated from immunohistochemistry data ($n = 5$/group). Values are presented as mean ± SEM, $n = 4$ independent biological replicates. (c) Quantitative gene expression showing robust neurotrophic activity of fetal MMC OSCs at 24 h based on brain-derived neurotrophic factor (*Bdnf*) and neurotrophin-4/5 (*Ntf4*) upregulation. Age-matched rat dorsal root ganglion (DRG) RNA was used as a positive control. Values are presented as mean ± SEM, $^*p \leq 0.01$ (Mann–Whitney), $n = 5$ independent biological replicates.

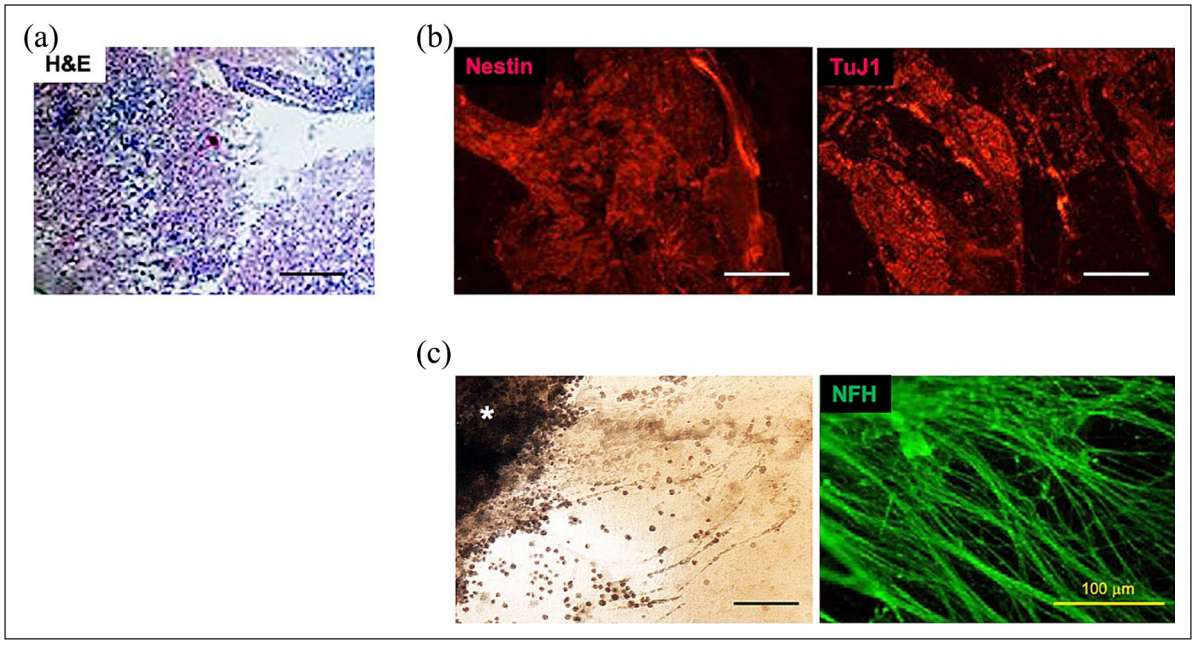

Figure 6. Maintenance of cytoarchitecture and progressive neurite growth of organotypic slices of MMC spinal cord in 3D hydrogels. (a) H&E staining of representative transverse slice after 7 days *in vitro* (E21 + 7) with hydrogel patch (magnification: 10×). Scale bar represents 100 mm. (b) Positive immunofluorescence staining of typical transverse E21 + 7 MMC slice using antibodies against nestin (left) and TuJ1 (right, Cy3 secondary, magnification: 20×). Scale bar represents 500 mm. (c) Representative light microscopy at the periphery of MMC slice (asterisk, left) with robust neurofilament (NFH)-positive staining of neurite extensions at E21 + 14 (right, FITC secondary, magnification: 40×). Scale bar represents 500 mm.

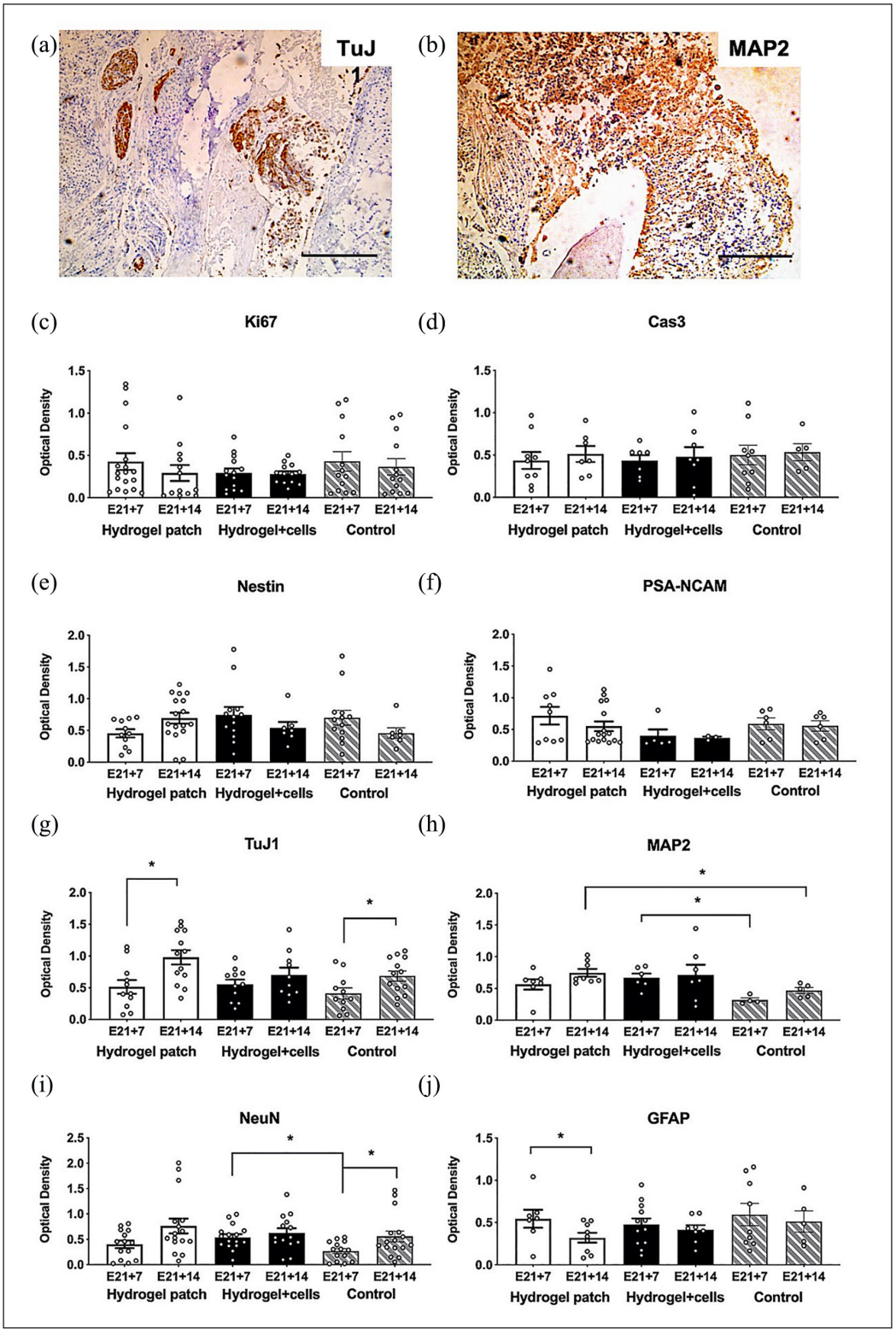

Figure 7. Quantitative histopathologic analysis of myelomeningocele organotypic slice cultures after hydrogel patch treatment (with or without neural progenitors) for 7 days (E21 + 7) or 14 days (E21 + 14). (a) and (b) Representative appearance of slice culture sections after staining using antibodies against TuJ1 and MAP2, respectively. Scale bar represents 500 mm. (c) and (d) Ki67 and Cas3 as markers of cell proliferation and apoptosis, respectively. Control slice cultures in media alone. (e) and (f) Nestin and PSA-NCAM to evaluate neural progenitor phenotypes. (g)–(i) TuJ1, MAP2, and NeuN as markers of neuronal cells. TuJ1 was significantly increased in E21 + 14 hydrogels without cells. (j) GFAP to evaluate astrocytes. GFAP was significantly decreased in E21 + 14 hydrogels without cells. Optical density values are presented as mean ± SEM, $*p \leq 0.05$ (Kruskal–Wallis), $n = 4$–13 independent biological replicates.

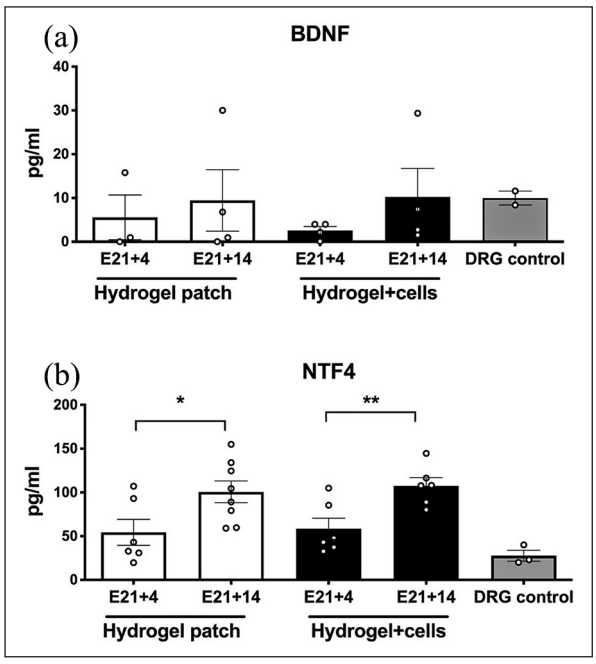

Figure 8. Neurotrophic activity as measured by enzyme-linked immunosorbent assay within myelomeningocele organotypic slice cultures after hydrogel patch treatment (with or without neural cells) for 4 days (E21 + 4) or 14 days (E21 + 14). (a) There was a trend toward increased brain-derived neurotrophic factor (BDNF) over time and a significant increase at E21 + 14 in organotypic slice cultures treated with hydrogel and neural cells when compared to E21 + 4. Age-matched rat dorsal root ganglion (DRG) cells were used as a positive control, $n = 4$ independent biological replicates. (b) There was a similar trend toward increased neurotrophin-4/5 (NTF4) levels over time. Values are presented as mean ± SEM, $*p \leq 0.05$ and $**p \leq 0.01$ (Mann–Whitney), $n = 4$ independent biological replicates.

E21 + 4: 58.5 ± 12.0, $p = 0.0152$; Figure 8). These neurotrophic factor levels were comparable to those from positive control dorsal root ganglion cells grown in 2D culture.

Discussion

In 2011, a landmark multi-institutional randomized trial was published demonstrating the efficacy of open surgical repair in human MMC fetuses.[4] Despite the promising clinical results associated with prenatal repair, bowel and bladder control continue to be ongoing challenges for these children, and more than half with spina bifida still cannot ambulate independently despite *in utero* repair.[25–27] Accordingly, novel experimental approaches aimed at further improving neurologic outcomes in these children have been pursued by multiple laboratories worldwide.[28–30]

In this study, we developed an injectable hydrogel patch containing human neural progenitor cells as proof of concept for a cell-based tissue engineering strategy for fetal MMC repair. The immature human neural progenitors generated using transgene-free reprogramming methods stained positive for nestin, remained mostly viable within 3D scaffolds for over 24 h, and expressed genes associated with neurotrophic activity. Although neural progenitors derived from human amniotic fluid could potentially be used as an "off-the-shelf" cell therapy product for affected fetuses at the time of repair, autologous use of these patches may also be possible given that amniotic fluid itself could easily be obtained upon prenatal diagnosis, which usually occurs by ultrasound at 18–20 weeks of gestation.[31,32] An autologous approach would have the additional advantage of alleviating concerns regarding the allogeneic immune rejection of donor cells. Currently, the time required for the preparation of our human neural progenitors took 10–12 weeks from amniotic fluid, but more rapid differentiation protocols from pluripotent stem cells have been described.[33,34] In addition, transdifferentiation of amniocytes into the neurogenic lineage and isolation of specific neurogenic cell populations that may be uniquely accessible in the MMC fetus may be viable alternatives for use in hydrogel patches.[35–38]

Our rationale for selecting neural progenitors as the ideal cell type for the MMC patch was based on previous work showing that neural progenitors can improve axonal regeneration in both animal and slice culture models of adult spinal cord injury.[39–42] In addition to neural progenitor differentiation into neurons, the functional multipotency of these cells, including host cell integration, re-myelination of host neuronal circuitry, and constitutive secretion of neurotrophic and neuroprotective factors responsible for regrowth and axonal regeneration, has been demonstrated.[43–46] However, in models of MMC, the use of cells derived from neural lineages to enhance spinal cord regeneration has been much more limited.[6,47] Unique aspects of the MMC spinal cord compared to those in other types of spinal cord injuries include the potential ability to intervene with treatment in a more permissive fetal environment and more chronic nature of the neural tube injury. The latter is thought to be secondary to a primary neurulation defect combined with ongoing mechanical and chemical trauma incurred with the absence of overlying soft tissue. Due to their potential to engraft and to support endogenous neural cells within the host through immunomodulatory and trophic factors, the utility of mesenchymal stem cells has been more thoroughly investigated and has been beneficial in some MMC models of repair.[39,48–52]

The second major finding from our study is the successful establishment of an organotypic model specific to the affected lumbar spinal cord in fetal MMC. Specifically, slice cultures from MMC pups demonstrated robust survival of endogenous cells within fibrin hydrogels for up to 14 days and showed evidence of continued differentiation into mature neuronal phenotypes with robust neurite outgrowth along its periphery. *Ex vivo* slice culture models of spinal cord regeneration have been widely embraced by neuroscientists as an informative research tool for over a decade.[22,53–57] In our study, we also found minimal glial responses after hydrogel treatment, which is not a trivial

finding given that previous histopathologic studies of the MMC placode have shown a paucity of mature neurons but with more extensive gliosis and fibrosis consistent with secondary injury.[58,59]

The MMC slice culture model is relatively simple to establish, easy to reproduce, and convenient for observing real-time changes in fetal spinal cord repair and regeneration. Further investigations in this model should allow us to test the effect of different neuroregenerative biomaterials and cell populations on different stages of development of the MMC spinal cord in a more controlled setting than what has been previously attempted.[60] In contrast, *in vivo* fetal surgical manipulations in both rodents and sheep are often tedious to perform and are associated with high fetal morbidity and mortality.[7,12] *Ex utero* murine embryo culture has also been described as a model of fetal treatment,[61] but this technique is limited by the short time window (e.g., less than 24 h) between intervention and demise.

Although our data suggest that fibrin hydrogels can support neuronal maturation over time, the addition of neural progenitors to the model did not consistently improve the regeneration of slice culture tissue. These results are in contrast to previous *in vivo* work in a prenatal ovine model, suggesting that the addition of bioactive fetal-derived cells may have benefit when compared to scaffold alone.[47] Given our cell viability data and relatively short time frame of *ex vivo* culture, it is also possible that the number of neural progenitors delivered was insufficient to demonstrate functional multipotency within the MMC spinal cord. Whether there may be a pruning effect of fibrin hydrogels on donor neural progenitors is unknown. However, we should also acknowledge that the MMC spinal cord used in our experiments was harvested near term (E21), which does not take advantage of the likely enhanced regenerative capacity of the spinal cord earlier in gestation.[62,63] Some investigators have suggested that donor cells may be more likely to differentiate into neural lineages within an embryonic spinal cord niche (E16).[49]

To date, most biomaterials described in animal models of MMC have comprised acellular, biodegradable sponges, sheets, or films whose primary aim is to provide tissue coverage over the spinal cord.[7,64–66] The choice of polymerizing hydrogels in our study was based on prior reports of their use in other neurogeneration models.[67–69] We and others have also shown that fibrin supports neural progenitor survival *in vivo*[16,70,71] and can provide physical and trophic support for nervous tissue ingrowth in neural tissue engineering models.[72,73] The safety and efficacy of fibrin glue (Tisseell; Baxter, Deerfield, IL) as a watertight sealant in neurosurgical applications have already been established,[74] and the potential of fibrin hydrogels as a delivery vehicle for donor neural cells and growth factors represents another advantage as a substrate for MMC repair.[75,76] Desirable properties for any hydrogel suitable for fetal MMC surgical repair include rapid transition from liquid to solid phase, impermeability in the aqueous *in utero* environment, favorable attachment to surrounding tissues, and biocompatibility with fetal neural elements.[5,61,77,78] In addition, the ideal hydrogel product should be injectable and capable of filling any cavity defects specific to the fetus, thereby providing a scaffolding to bridge damaged axons within the spinal cord.[79]

One drawback of fibrin hydrogels has been the rapid degradation by native plasmin over the first several weeks after application.[80,81] Although modifying the chemical properties of our hydrogels may extend its degradation until there is complete ingrowth of adjacent epithelium, another strategy to circumvent short degradation times would be to employ a biodegradable sheet on top of the hydrogel patch. This bi-layered approach could also serve an important barrier function to further minimize mechanical trauma.[30,82] Continued advances in the evaluation of these biomaterials may eventually enable more widespread adoption of fetoscopic repair of MMC defects, which remains technically demanding compared to open surgery but has been shown to induce less maternal–fetal morbidity.[83,84]

Moving forward, we propose that our slice culture model could be used as a unique "disease-in-dish" approach to understand mechanisms of mechanical and chemical spinal cord injury in MMC. The direct and paracrine effects of neural stem cells on the fetal spinal cord remain essentially unknown,[47] and techniques for long-term experiments using spinal cord slice cultures have only recently been described.[14] Since there remains a paucity of well-established biomimetic models that permit effective *in vitro* screening of fetal spinal cord regeneration,[85] our approach represents a novel, high-throughput platform for evaluating next-generation MMC repair strategies, including stem cells and bioactive molecules, in both the prenatal and postnatal setting. Other stem cell populations, neurotrophins, and growth factors could be screened to better identify the optimal microenvironment to facilitate neural regeneration in this condition.

Despite the results presented herein, there are several important caveats and limitations that should be acknowledged. First, as with most animal models produced using teratogenic compounds, there is inherent heterogeneity in the degree of spinal cord damage in the retinoic acid model of MMC. Such differences may explain some of the variability in our slice culture assays. Second, until we accumulate long-term data from slice cultures, we have yet to quantify neurite extension as a marker for degree of axonal regeneration and neural networking capacity. Such data may also allow us to measure functional aspects within these slice culture models as described by others.[86,87] Third, we did not utilize baseline control groups that include direct exposure of our constructs *ex vivo* to culture media containing amniotic fluid. While not essential to demonstrate the biocompatibility of hydrogels in our model, inclusion of these groups would be ideal to better mimic the *in vivo*

environment where the neural tube defect remains in contact with amniotic fluid.[88,89] Such studies may also allow us to assess neural inflammation and the role of microglia during tissue regeneration. Finally, findings within this small animal model may be species-specific and therefore would likely require subsequent validation in scale-up studies on human tissues prior to clinical translation.

Conclusion

In summary, we developed hydrogel surgical patches for use during prenatal spina bifida repair and demonstrated viability of both human and rat neural progenitor donor cells within this 3D microenvironment. The patches were then tested in a 14-day organotypic slice culture model, which demonstrated ongoing neuronal development, neurite extension, limited astrocytosis, and robust neurotrophin activity. Thus, these experiments reveal the biocompatibility of fibrin hydrogel patches within the fetal MMC spinal cord and suggest an *ex vivo* organotypic system as a useful tool for evaluating mechanisms of damage and repair in children with neural tube defects.

Acknowledgements

The authors would like to thank Fabio Triolo, DdR, MPhil, PhD, and Charles S Cox, MD (University of Texas, Houston), for human amniotic fluid specimens and K. Sue O'Shea, PhD (University of Michigan), for guidance on cell reprogramming and neural progenitor cell differentiation.

Declaration of conflicting interests

The author(s) declared no potential conflicts of interest with respect to the research, authorship, and/or publication of this article.

Funding

The author(s) disclosed receipt of the following financial support for the research, authorship, and/or publication of this article: Funding for this project was made possible by grants from the National Institutes of Health (R01EBB005678 (L.D.S.) and R01HD091323 (S.M.K.)).

ORCID iD

Shaun M Kunisaki https://orcid.org/0000-0002-9229-4733

Supplemental material

Supplemental material for this article is available online.

References

1. Bowman RM and McLone DG. Neurosurgical management of spina bifida: research issues. *Dev Disabil Res Rev* 2010; 16(1): 82–87.
2. Heffez DS, Aryanpur J, Hutchins GM, et al. The paralysis associated with myelomeningocele: clinical and experimental data implicating a preventable spinal cord injury. *Neurosurgery* 1990; 26(6): 987–992.
3. Meuli M, Meuli-Simmen C, Hutchins GM, et al. In utero surgery rescues neurological function at birth in sheep with spina bifida. *Nat Med* 1995; 1(4): 342–347.
4. Adzick NS, Thom EA, Spong CY, et al. A randomized trial of prenatal versus postnatal repair of myelomeningocele. *N Engl J Med* 2011; 364: 993–1004.
5. Watanabe M, Kim AG and Flake AW. Tissue engineering strategies for fetal myelomeningocele repair in animal models. *Fetal Diagn Ther* 2015; 37(3): 197–205.
6. Fauza DO, Jennings RW, Teng YD, et al. Neural stem cell delivery to the spinal cord in an ovine model of fetal surgery for spina bifida. *Surgery* 2008; 144(3): 367–373.
7. Watanabe M, Jo J, Radu A, et al. A tissue engineering approach for prenatal closure of myelomeningocele with gelatin sponges incorporating basic fibroblast growth factor. *Tissue Eng Part A* 2010; 16(5): 1645–1655.
8. Wang A, Brown EG, Lankford L, et al. Placental mesenchymal stromal cells rescue ambulation in ovine myelomeningocele. *Stem Cells Transl Med* 2015; 4(6): 659–669.
9. Farrelly JS, Bianchi AH, Ricciardi AS, et al. Alginate microparticles loaded with basic fibroblast growth factor induce tissue coverage in a rat model of myelomeningocele. *J Pediatr Surg* 2019; 54(1): 80–85.
10. Danzer E, Schwarz U, Wehrli S, et al. Retinoic acid induced myelomeningocele in fetal rats: characterization by histopathological analysis and magnetic resonance imaging. *Exp Neurol* 2005; 194(2): 467–475.
11. Vanover M, Pivetti C, Galganski L, et al. Spinal angulation: a limitation of the fetal lamb model of myelomeningocele. *Fetal Diagn Ther* 2019; 46(6): 376–384.
12. Galganski LA, Yamashiro KJ, Pivetti CD, et al. A decade of experience with the ovine model of myelomeningocele: risk factors for fetal loss. *Fetal Diagn Ther* 2020; 47(6): 507–513.
13. Stoppini L, Buchs PA and Muller D. A simple method for organotypic cultures of nervous tissue. *J Neurosci Methods* 1991; 37(2): 173–182.
14. Liu JJ, Huang YJ, Xiang L, et al. A novel method of organotypic spinal cord slice culture in rats. *Neuroreport* 2017; 28: 1097–1102.
15. des Rieux A, Shikanov A and Shea LD. Fibrin hydrogels for non-viral vector delivery in vitro. *J Control Release* 2009; 136: 148–154.
16. Johnson PJ, Parker SR and Sakiyama-Elbert SE. Fibrin-based tissue engineering scaffolds enhance neural fiber sprouting and delay the accumulation of reactive astrocytes at the lesion in a subacute model of spinal cord injury. *J Biomed Mater Res A* 2010; 92(1): 152–163.
17. Johnson PJ, Tatara A, Shiu A, et al. Controlled release of neurotrophin-3 and platelet-derived growth factor from fibrin scaffolds containing neural progenitor cells enhances survival and differentiation into neurons in a subacute model of SCI. *Cell Transplant* 2010; 19(1): 89–101.
18. Kunisaki SM, Armant M, Kao GS, et al. Tissue engineering from human mesenchymal amniocytes: a prelude to clinical trials. *J Pediatr Surg* 2007; 42(6): 974–979, discussion 979.
19. Jiang G, Di Bernardo J, Maiden MM, et al. Human transgene-free amniotic-fluid-derived induced pluripotent stem cells for autologous cell therapy. *Stem Cells Dev* 2014; 23: 2613–2625.

20. Ruifrok AC and Johnston DA. Quantification of histochemical staining by color deconvolution. *Anal Quant Cytol Histol* 2001; 23: 291–299.
21. Bijlsma MF, Leenders PJ, Janssen BJ, et al. Endogenous hedgehog expression contributes to myocardial ischemia-reperfusion-induced injury. *Exp Biol Med* 2008; 233(8): 989–996.
22. Kamei N, Tanaka N, Oishi Y, et al. BDNF, NT-3, and NGF released from transplanted neural progenitor cells promote corticospinal axon growth in organotypic cocultures. *Spine* 1976; 200732: 1272–1278.
23. Ji XC, Dang YY, Gao HY, et al. Local injection of Lenti-BDNF at the lesion site promotes M2 macrophage polarization and inhibits inflammatory response after spinal cord injury in mice. *Cell Mol Neurobiol* 2015; 35(6): 881–890.
24. Neumann H, Misgeld T, Matsumuro K, et al. Neurotrophins inhibit major histocompatibility class II inducibility of microglia: involvement of the p75 neurotrophin receptor. *Proc Natl Acad Sci U S A* 1998; 95: 5779–5784.
25. Farmer DL, Thom EA, Brock JW 3rd, et al. The management of myelomeningocele study: full cohort 30-month pediatric outcomes. *Am J Obstet Gynecol* 2018; 218(2): 256.e1–256.e2.
26. Danzer E, Thomas NH, Thomas A, et al. Long-term neurofunctional outcome, executive functioning, and behavioral adaptive skills following fetal myelomeningocele surgery. *Am J Obstet Gynecol* 2016; 214(2): 269.e2–269.e2.
27. Danzer E, Joyeux L, Flake AW, et al. Fetal surgical intervention for myelomeningocele: lessons learned, outcomes, and future implications. *Dev Med Child Neurol* 2020; 62(4): 417–425.
28. Bardill JR, Park D and Marwan AI. Improved coverage of mouse myelomeningocele with a mussel inspired reverse thermal gel. *J Surg Res* 2020; 251: 262–274.
29. Fontecha CG, Peiro JL, Sevilla JJ, et al. Fetoscopic coverage of experimental myelomeningocele in sheep using a patch with surgical sealant. *Eur J Obstet Gynecol Reprod Biol* 2011; 156(2): 171–176.
30. Tatu R, Oria M, Pulliam S, et al. Using poly(L-lactic acid) and poly(varepsilon-caprolactone) blends to fabricate self-expanding, watertight and biodegradable surgical patches for potential fetoscopic myelomeningocele repair. *J Biomed Mater Res B Appl Biomater* 2019; 107: 295–305.
31. Kaviani A, Guleserian K, Perry TE, et al. Fetal tissue engineering from amniotic fluid. *J Am Coll Surg* 2003; 196: 592–597.
32. Kunisaki SM. Amniotic fluid stem cells for the treatment of surgical disorders in the fetus and neonate. *Stem Cells Transl Med* 2018; 7(11): 767–773.
33. Chambers SM, Fasano CA, Papapetrou EP, et al. Highly efficient neural conversion of human ES and iPS cells by dual inhibition of SMAD signaling. *Nat Biotechnol* 2009; 27(3): 275–280.
34. Yan Y, Shin S, Jha BS, et al. Efficient and rapid derivation of primitive neural stem cells and generation of brain subtype neurons from human pluripotent stem cells. *Stem Cells Transl Med* 2013; 2(11): 862–870.
35. Prusa AR, Marton E, Rosner M, et al. Neurogenic cells in human amniotic fluid. *Am J Obstet Gynecol* 2004; 191: 309–314.
36. Marotta M, Fernández-Martín A, Oria M, et al. Isolation, characterization, and differentiation of multipotent neural progenitor cells from human cerebrospinal fluid in fetal cystic myelomeningocele. *Stem Cell Res* 2017; 22: 33–42.
37. Pennington EC, Gray FL, Ahmed A, et al. Targeted quantitative amniotic cell profiling: a potential diagnostic tool in the prenatal management of neural tube defects. *J Pediatr Surg* 2013; 48(6): 1205–1210.
38. Pennington EC, Rialon KL, Dionigi B, et al. The impact of gestational age on targeted amniotic cell profiling in experimental neural tube defects. *Fetal Diagn Ther* 2015; 37(1): 65–69.
39. Cho JS, Park HW, Park SK, et al. Transplantation of mesenchymal stem cells enhances axonal outgrowth and cell survival in an organotypic spinal cord slice culture. *Neurosci Lett* 2009; 454: 43–48.
40. Nori S, Okada Y, Yasuda A, et al. Grafted human-induced pluripotent stem-cell-derived neurospheres promote motor functional recovery after spinal cord injury in mice. *Proc Natl Acad Sci U S A* 2011; 108: 16825–16830.
41. Vroemen M, Aigner L, Winkler J, et al. Adult neural progenitor cell grafts survive after acute spinal cord injury and integrate along axonal pathways. *Eur J Neurosci* 2003; 18(4): 743–751.
42. Hamasaki T, Tanaka N, Kamei N, et al. Magnetically labeled neural progenitor cells, which are localized by magnetic force, promote axon growth in organotypic cocultures. *Spine* 1976; 200732: 2300–2305.
43. Hooshmand MJ, Sontag CJ, Uchida N, et al. Analysis of host-mediated repair mechanisms after human CNS-stem cell transplantation for spinal cord injury: correlation of engraftment with recovery. *PLoS ONE* 2009; 4: e5871.
44. Cummings BJ, Uchida N, Tamaki SJ, et al. Human neural stem cell differentiation following transplantation into spinal cord injured mice: association with recovery of locomotor function. *Neurol Res* 2006; 28(5): 474–481.
45. Hawryluk GW, Mothe A, Wang J, et al. An in vivo characterization of trophic factor production following neural precursor cell or bone marrow stromal cell transplantation for spinal cord injury. *Stem Cells Dev* 2012; 21: 2222–2238.
46. Teng YD. Functional multipotency of stem cells: biological traits gleaned from neural progeny studies. *Semin Cell Dev Biol* 2019; 95: 74–83.
47. Saadai P, Wang A, Nout YS, et al. Human induced pluripotent stem cell-derived neural crest stem cells integrate into the injured spinal cord in the fetal lamb model of myelomeningocele. *J Pediatr Surg* 2013; 48(1): 158–163.
48. Lankford L, Chen YJ, Saenz Z, et al. Manufacture and preparation of human placenta-derived mesenchymal stromal cells for local tissue delivery. *Cytotherapy* 2017; 19(6): 680–688.
49. Li H, Gao F, Ma L, et al. Therapeutic potential of in utero mesenchymal stem cell (MSCs) transplantation in rat foetuses with spina bifida aperta. *J Cell Mol Med* 2012; 16(7): 1606–1617.
50. Vanover M, Pivetti C, Lankford L, et al. High density placental mesenchymal stromal cells provide neuronal preservation and improve motor function following in utero treatment of ovine myelomeningocele. *J Pediatr Surg* 2019; 54(1): 75–79.

51. Chen YJ, Chung K, Pivetti C, et al. Fetal surgical repair with placenta-derived mesenchymal stromal cell engineered patch in a rodent model of myelomeningocele. *J Pediatr Surg*. Epub ahead of print 12 October 2017. DOI: 10.1016/j.jpedsurg.2017.10.040
52. Cao S, Wei X, Li H, et al. Comparative study on the differentiation of mesenchymal stem cells between fetal and postnatal rat spinal cord niche. *Cell Transplant* 2016; 25(6): 1115–1130.
53. Cifra A, Mazzone GL, Nani F, et al. Postnatal developmental profile of neurons and glia in motor nuclei of the brainstem and spinal cord, and its comparison with organotypic slice cultures. *Dev Neurobiol* 2012; 72(8): 1140–1160.
54. Sypecka J, Koniusz S, Kawalec M, et al. The organotypic longitudinal spinal cord slice culture for stem cell study. *Stem Cells Int* 2015; 2015: 471216.
55. Bonnici B and Kapfhammer JP. Spontaneous regeneration of intrinsic spinal cord axons in a novel spinal cord slice culture model. *Eur J Neurosci* 2008; 27(10): 2483–2492.
56. Schizas N, Rojas R, Kootala S, et al. Hyaluronic acid-based hydrogel enhances neuronal survival in spinal cord slice cultures from postnatal mice. *J Biomater Appl* 2014; 28(6): 825–836.
57. Mazzone GL and Nistri A. Delayed neuroprotection by riluzole against excitotoxic damage evoked by kainate on rat organotypic spinal cord cultures. *Neuroscience* 2011; 190: 318–327.
58. George TM and Cummings TJ. The immunohistochemical profile of the myelomeningocele placode: is the placode normal. *Pediatr Neurosurg* 2003; 39(5): 234–239.
59. Reis JL, Correia-Pinto J, Monteiro MP, et al. Immunocytochemical characterization of astrocytosis along the spinal cord of loop-tail/curly-tail mice with myelomeningocele. *Pediatr Neurosurg* 2008; 44(4): 288–295.
60. Turner CG, Pennington EC, Gray FL, et al. Intra-amniotic delivery of amniotic-derived neural stem cells in a syngeneic model of spina bifida. *Fetal Diagn Ther* 2013; 34(1): 38–43.
61. Marwan AI, Williams SM, Bardill JR, et al. Reverse thermal gel for in utero coverage of spina bifida defects: an innovative bioengineering alternative to open fetal repair. *Macromol Biosci* 2017; 17(6): 473.
62. Zieba J, Miller A, Gordiienko O, et al. Clusters of amniotic fluid cells and their associated early neuroepithelial markers in experimental myelomeningocele: correlation with astrogliosis. *PLoS ONE* 2017; 12(3): e0174625.
63. Shen J, Zhou G, Chen H, et al. Morphology of nervous lesion in the spinal cord and bladder of fetal rats with myelomeningocele at different gestational age. *J Pediatr Surg* 2013; 48(12): 2446–2452.
64. Saadai P, Nout YS, Encinas J, et al. Prenatal repair of myelomeningocele with aligned nanofibrous scaffolds—a pilot study in sheep. *J Pediatr Surg* 2011; 46(12): 2279–2283.
65. Watanabe M, Li H, Kim AG, et al. Complete tissue coverage achieved by scaffold-based tissue engineering in the fetal sheep model of Myelomeningocele. *Biomaterials* 2016; 76: 133–143.
66. Papanna R, Mann LK, Snowise S, et al. Neurological outcomes after human umbilical cord patch for in utero spina bifida repair in a sheep model. *AJP Rep* 2016; 6(3): e309–e317.
67. Gerardo-Nava J, Hodde D, Katona I, et al. Spinal cord organotypic slice cultures for the study of regenerating motor axon interactions with 3D scaffolds. *Biomaterials* 2014; 35(14): 4288–4296.
68. Cigognini D, Satta A, Colleoni B, et al. Evaluation of early and late effects into the acute spinal cord injury of an injectable functionalized self-assembling scaffold. *PLoS ONE* 2011; 6(5): e19782.
69. Montgomery A, Wong A, Gabers N, et al. Engineering personalized neural tissue by combining induced pluripotent stem cells with fibrin scaffolds. *Biomater Sci* 2015; 3(2): 401–413.
70. Lu P, Graham L, Wang Y, et al. Promotion of survival and differentiation of neural stem cells with fibrin and growth factor cocktails after severe spinal cord injury. *J Vis Exp* 2014; 89: e50641.
71. Lu P, Jones LL, Snyder EY, et al. Neural stem cells constitutively secrete neurotrophic factors and promote extensive host axonal growth after spinal cord injury. *Exp Neurol* 2003; 181(2): 115–129.
72. De Laporte L, Yan AL and Shea LD. Local gene delivery from ECM-coated poly(lactide-co-glycolide) multiple channel bridges after spinal cord injury. *Biomaterials* 2009; 30(12): 2361–2368.
73. King VR, Alovskaya A, Wei DY, et al. The use of injectable forms of fibrin and fibronectin to support axonal ingrowth after spinal cord injury. *Biomaterials* 2010; 31(15): 4447–4456.
74. Jeon SH, Lee SH, Tsang YS, et al. Watertight sealing without lumbar drainage for incidental ventral dural defect in transthoracic spine surgery: a retrospective review of 53 cases. *Clin Spine Surg* 2017; 30(6): E702–E706.
75. Willerth SM, Rader A and Sakiyama-Elbert SE. The effect of controlled growth factor delivery on embryonic stem cell differentiation inside fibrin scaffolds. *Stem Cell Res* 2008; 1(3): 205–218.
76. Silva J, Bento AR, Barros D, et al. Fibrin functionalization with synthetic adhesive ligands interacting with alpha6beta1 integrin receptor enhance neurite outgrowth of embryonic stem cell-derived neural stem/progenitors. *Acta Biomater* 2017; 59: 243–256.
77. Winkler SM, Harrison MR and Messersmith PB. Biomaterials in fetal surgery. *Biomater Sci* 2019; 7: 3092–3109.
78. Vu T, Mann LK, Fletcher SA, et al. Suture techniques and patch materials using an in-vitro model for watertight closure of in-utero spina bifida repair. *J Pediatr Surg* 2020; 55(4): 726–731.
79. Yao S, Yu S, Cao Z, et al. Hierarchically aligned fibrin nanofiber hydrogel accelerated axonal regrowth and locomotor function recovery in rat spinal cord injury. *Int J Nanomedicine* 2018; 13: 2883–2895.
80. Tukmachev D, Forostyak S, Koci Z, et al. Injectable extracellular matrix hydrogels as scaffolds for spinal cord injury repair. *Tissue Eng Part A* 2016; 22(3–4): 306–317.
81. Iwaya K, Mizoi K, Tessler A, et al. Neurotrophic agents in fibrin glue mediate adult dorsal root regeneration into spinal cord. *Neurosurgery* 1999; 44(3): 589–595, discussion 595.

82. Peiro JL, Fontecha CG, Ruano R, et al. Single-access fetal endoscopy (SAFE) for myelomeningocele in sheep model I: amniotic carbon dioxide gas approach. *Surg Endosc* 2013; 27(10): 3835–3840.
83. Sanz Cortes M, Lapa DA, Acacio GL, et al. Proceedings of the first annual meeting of the international fetoscopic myelomeningocele repair consortium. *Ultrasound Obstet Gynecol* 2019; 53(6): 855–863.
84. Hii LY, Sung CA and Shaw SW. Fetal surgery and stem cell therapy for meningomyelocele. *Curr Opin Obstet Gynecol* 2020; 32(2): 147–151.
85. Galganski LA, Kumar P, Vanover MA, et al. In utero treatment of myelomeningocele with placental mesenchymal stromal cells—selection of an optimal cell line in preparation for clinical trials. *J Pediatr Surg*. Epub ahead of print 21 October 2019. DOI: 10.1016/j.jpedsurg.2019.09.029
86. Magloire V and Streit J. Intrinsic activity and positive feedback in motor circuits in organotypic spinal cord slice cultures. *Eur J Neurosci* 2009; 30(8): 1487–1497.
87. Pandamooz S, Nabiuni M, Miyan J, et al. Organotypic spinal cord culture: a proper platform for the functional screening. *Mol Neurobiol* 2016; 53(7): 4659–4674.
88. Pandamooz S, Salehi MS, Zibaii MI, et al. Epidermal neural crest stem cell-derived glia enhance neurotrophic elements in an ex vivo model of spinal cord injury. *J Cell Biochem* 2018; 119(4): 3486–3496.
89. Drewek MJ, Bruner JP, Whetsell WO, et al. Quantitative analysis of the toxicity of human amniotic fluid to cultured rat spinal cord. *Pediatr Neurosurg* 1997; 27(4): 190–193.